International Journal of Applied Engineering Research ISSN 0973-4562 Volume 14, Number 11 (2019) pp. 2622-2629


# Coupled dynamic model for a mobile manipulator

**V. Prada-Jiménez**[1,2], **P. A. Niño-Suárez**[3], **M. F. Mauledoux-Monroy**[4] **and J. A. Aponte-Rodríguez**[5].

[1]*Assistant Professor, Department of Electronics Engineering, Universidad Central. Cl. 21 #4-40. Bogotá, Colombia.*

[2]*Assistant Professor, Instituto Politécnico Nacional - CIDETEC. Av. Juan de Dios Bátiz, Santo Tomas, 07738. Ciudad de México, México.*

[3]*Assistant Professor, Instituto Politécnico Nacional - ESIME. Av. De las Granjas 682, Santo Tomas, 02519. Ciudad de México, México.*

[4]*Assistant Professor, Department of Mechatronics Engineering, Universidad Militar Nueva Granada. Cr. 11 #101-80. Bogotá, Colombia.*

[5]*Assistant Professor, Department of Mechatronics Engineering, Universidad Militar Nueva Granada. Cr. 11 #101-80. Bogotá, Colombia.*

**Abstract**
Currently, there is great interest in obtaining the coupled dynamic model of mobile manipulators and the main reason is because this model allows to efficiently control the trajectory of the final effector. Therefore, this article presents a methodology to obtain the coupled dynamic model of a mobile platform differential type and an anthropomorphic manipulator of 3 degrees of freedom. The coupled dynamic model allows the calculation of the necessary torques of each of the joints, both mobile and manipulator, to follow the desired path of the end effector. The results of the simulation are presented and show both mathematically and graphically that the dynamic model obtained is coupled.

**Keywords:** Anthropomorphic, Coupled, Differential, Kinematic, Dynamic, Manipulator, Mobile, Non-holonomic.

## Introduction

Robotic manipulators are usually installed on a fixed base and with a limited workspace. However, due to the diversity of tasks that currently arise, it is necessary to expand the work spaces, which is why it is common to add conveyor belts, transport devices, and choose to use Mobile Manipulators (MM) in some cases. MM have many potential applications due to the capabilities, some of them are present in manufacturing, assembly, construction, explosives neutralization, nuclear reactors maintenance, and the planets exploration [1].

A MM consists of a manipulators assembled on top of a mobile platform or mobile robot [2]. This has a considerably larger workspace than a fixed manipulator and greater manipulation than mobile robots. Further, combines the manipulation capacity offered by fixed-base manipulators and the mobility offered by mobile platforms. By being able to perform both tasks simultaneously, the MM has advantages over stationary manipulators, such as a greater work space and greater autonomy by being wireless.

In general, a MM can perform different types of tasks, of which locomotion and manipulation are highlighted. Usually, both tasks have been executed separately and consecutively. Therefore, the kinematic and dynamic modeling of the base and the manipulator arm are usually carried out independently even with different methodologies [3]–[5] and sometimes the coupling is not performed due to the complexity in the modeling regarding the non-holonomic restrictions [6]–[8].

Some examples of the possible configurations that can be implemented are the locomotion with wheels or paws and in the manipulation with arms of open or closed kinematics, making it necessary to determine the type of articulation and the number of Degrees of Freedom (DoF). A fundamental work for the modeling of mobile robots with wheels is presented in [7], where the mathematical model of four types of configurations is determined. A kinematic modeling scheme for mobile manipulators is presented in [9] and in [10], where the model of the mobile platform and the manipulator are determined separately. In [4] a method to couple the kinematic model of the mobile base with the one of the stationary manipulator is presented, but the mobile and the arm are modeled by different methods. In general, the Euler-Lagrange method is used as main tool to obtain the model, and the Lagrange multipliers to incorporate the non-holonomic constraints [11]; however, exist a depend on the kinematic model to incorporate the non-holonomic constraints.

Due to the usefulness of mobile manipulators, it is important to obtain kinematic and dynamic models that allow a quick and easy manipulator analysis. It is also important to have tools that build on existing knowledge and not having to use different methodologies for modeling each part of the MM. This allows to use simple control techniques and the possibility of implementing it in an embedded system.

Recently, papers describing complex methodologies for coupled kinematic and dynamic modeling have been published [3], [4], [6], [12]–[17]. These articles stablish yours methodologies for the coupling of MM based on [18].

The main objective of this work is to present a simple methodology to obtain the coupled dynamic model of an MM. The coupled model has the following advantages:

- It allows to use a single control technique and not separately mobile-manipulator as it is currently done.
- It facilitates the accomplishment of tasks of assembly and manipulation, because it realizes the calculation of the necessary torque by each actuator (motors of the wheels and motors of the articulations of the arm) with only to

establish the path of the effector and not separately mobile-manipulator as is currently done
- It allows the implementation in an embedded system due to its simplicity and thus make hardware in the loop or the pertinent validations.

This article is organized as follows, the first section presents the configuration of the MM to be modeled; the second section presents the methodology to be used for the dynamic MM model; the third section presents the mathematical description of a coupled dynamic model; the fourth and fifth sections present the model of the platform under non-holonomic restrictions; the sixth section presents the procedure to obtain the coupled dynamic model of the differential type mobile-robot and for the anthropomorphic type manipulator; the seventh section shows the implementation and results obtained. Finally, the conclusions and the bibliographical references used are presented.

**Conceptual design of the MM**

The selected robot has an anthropomorphic type manipulator, three links and three DoF. Each one of the DoF is given by an articulation of the rotational type. For the conceptual design of the mobile platform, a type (2.0) robot [6] was chosen. This platform has versatility of movement, ease in modeling and in the action of control. The robot has two fixed wheels and mobility is achieved by having a different speed on each wheel, which is called differential locomotion. The robot has a third passive wheel that is used to give stability and serve as a point of support. The conceptual design of the MM is presented in Figure 1.

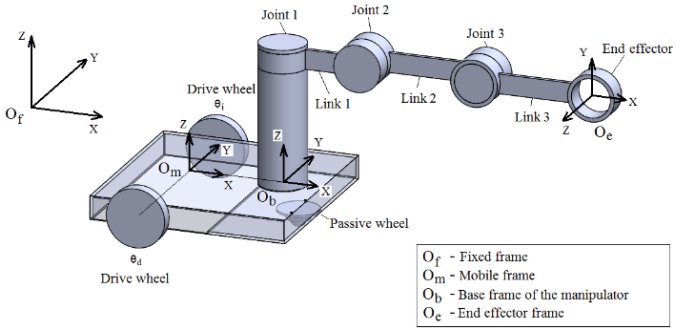


**Figure 1.** Conceptual design of the MM driven by differential system.

**Dynamic of mobile manipulators**

In general, a MM consist of a sequence of rigid links connected by revolution or prismatic joints mounted on a mobile base. The mobile base could be separated as several wheels and a platform. Each wheel and the platform could be treated as one joint-link pair, and one link. The mobile platform has three DoF and the manipulators has a degree of freedom by each joint-link pair.

The dynamics of MM can be obtained from two different formulations: the closed-form Lagrange formulation and the Euler-forward-backward recursive formulation. The Lagrangian treats the MM as a single element and performs the analysis using the Lagrange function (the Lagrange function is the difference between the kinetic energy and the potential energy of the robotic system). Euler's approach describes the combined translational and rotational dynamics of a rigid body in respect of the center of mass of each link. The dynamics of the whole MM can be described by the recursive dynamic equations forward and backward. Therefore, two different types of formulations provide different points of view about the physical meaning of the dynamics but it is known that the model is unique.

In the Lagrange formulation, the equations of motion can be obtained systematically and independent of the coordinate system. Once the set of coordinates $\boldsymbol{q}_i$, $i = 1, \dots, n$ ($n$ is the DoF) or generalized coordinates is determined, the links which effectively describes the position of the manipulator is chosen. The Lagrangian of the mechanical system can be defined as a generalized coordinates function, see equation (1):

$$L = K - U \tag{1}$$

where $L$ is the Lagrange formulation that considers $K$ as the kinetic energy and $U$ as the potential energy of the system [19], [20]. The equation of motion for a conservative system is given by equation (2).

$$\tau_i = \frac{d}{dt}\frac{\partial L}{\partial \dot{\boldsymbol{q}}_i} - \frac{\partial L}{\partial \boldsymbol{q}_i} \tag{2}$$

where $\boldsymbol{q}$ is a vector of $n$ generalized coordinates, $\boldsymbol{q}_i$, $\boldsymbol{\tau}$ is a vector of $n$ generalized forces, and the Lagrangian is the difference between the kinetic energy and the potential energy. Dynamic analysis consists of finding the relation between the generalized coordinates $\boldsymbol{q}$ and the generalized forces $\boldsymbol{\tau}$. Therefore, most authors prefer a closed formulation of Lagrange, so as to facilitate the use of controllers and the analysis of the evolution of generalized coordinates [21]–[23].

**Mathematical description of coupled dynamics**

Consider a $n$-DoF manipulator mounted on a non-holonomic mobile platform. The dynamics of an MM consists of the coupled dynamics of the mobile platform and the manipulator subject to restrictions, see equation (3) [21]:

$$M(\boldsymbol{q})\ddot{\boldsymbol{q}} + C(\boldsymbol{q}, \dot{\boldsymbol{q}})\dot{\boldsymbol{q}} + \boldsymbol{G}(\boldsymbol{q}) = B(\boldsymbol{q})\boldsymbol{\tau} + \boldsymbol{F} \tag{3}$$

where $\boldsymbol{q} = [\boldsymbol{q}_v^T, \boldsymbol{q}_a^T]^T \in \Re^n$, $\boldsymbol{q}_v \in \Re_v^n$ describes the vector of generalized coordinates for the mobile platform; $\boldsymbol{q}_a \in \Re_a^n$ is the vector of generalized coordinates for the manipulator; and $n = n_a + n_v$; $M(\boldsymbol{q}) \in \Re^{n\times n}$ is the symmetric bounded positive definite inertia matrix, $C(\boldsymbol{q}, \dot{\boldsymbol{q}})\dot{\boldsymbol{q}} \in \Re^n$ expresses the centripetal and Coriolis torques; $G(\boldsymbol{q}) \in \Re^n$ is the gravitational torque vector; $B(\boldsymbol{q}) \in \Re^{n\times k}$ is a full-range input transformation matrix; $\boldsymbol{\tau} \in \Re^k$ is the vector of control input; $\boldsymbol{F} = J^T\boldsymbol{\lambda} \in \Re^n$ denotes the vector of constraint forces with $J(\boldsymbol{q}) = [A, 0]$ and $\boldsymbol{\lambda} = [\boldsymbol{\lambda}_n, 0]^T$ for non-holonomic constraints of the system. Since $A^T(\boldsymbol{q}_v) \in \Re^{n_v\times(n_v-m)}$, and the range of $A$ is $n_v - m$, it is always possible to find a $m + n_a$ matrix of rank $R(\boldsymbol{q}) \in \Re^{n\times m}$ formed by a set of smooth and linearly independent vector fields spinning the null space of $J(\boldsymbol{q})$, as it is presented in (4).

$$R^T(\boldsymbol{q})J^T(\boldsymbol{q}) = 0 \quad (4)$$

Note that $R(\boldsymbol{q}) = [r_1(\boldsymbol{q}_v), \dots, r_m(\boldsymbol{q}_v), r_a(\boldsymbol{q}_v)]$ and defines an auxiliary function in time $\dot{\boldsymbol{\eta}}(t) = [\dot{\boldsymbol{\eta}}_1(t), \dots, \dot{\boldsymbol{\eta}}_m(t), \dot{\boldsymbol{\eta}}_a(t)]^T \in \Re^m$ such that

$$\dot{\boldsymbol{q}} = R(\boldsymbol{q})\dot{\boldsymbol{\eta}}(t) = r_1(\boldsymbol{q}_v)\dot{\boldsymbol{\eta}}_1(t) + \cdots + r_m(\boldsymbol{q}_v)\dot{\boldsymbol{\eta}}_m(t) + r_a(\boldsymbol{q}_v)\dot{\boldsymbol{\eta}}_a(t) \quad (5)$$

Equation (5) is the so-called kinetic model of non-holonomic systems in the literature. In general, $\dot{\boldsymbol{\eta}}(t)$ has a physical meaning, consisting of the linear velocity $v$, the angular velocity $w$ and the velocity of the $q_a$, that is, define $\dot{\boldsymbol{\eta}}(t) = [v \quad w \quad q_a]^T$. Equation (5) describes the kinematic relationship between the motion vector $\boldsymbol{q}(t)$ and the velocity vector $\dot{\boldsymbol{\eta}}(t)$. Differentiating (5) we have equation (6):

$$\ddot{\boldsymbol{q}} = \dot{R}(\boldsymbol{q})\dot{\boldsymbol{\eta}} + R(\boldsymbol{q})\ddot{\boldsymbol{\eta}} \quad (6)$$

of (5), $\dot{\boldsymbol{\eta}}$ can be obtained from $\boldsymbol{q}$ and $\dot{\boldsymbol{q}}$ as:

$$\dot{\boldsymbol{\eta}} = [R^T(\boldsymbol{q})R(\boldsymbol{q})]^{-1}R^T(\boldsymbol{q})\dot{\boldsymbol{q}} \quad (7)$$

Equation (3), which satisfies the non-holonomic constraint $A(\boldsymbol{q})\dot{\boldsymbol{q}} = 0$, can be rewritten in terms of the internal state variable $\dot{\boldsymbol{\eta}}$ by substituting equations (5) and (6) in (3), as presented in equation (8):

$$M(\boldsymbol{q})R(\boldsymbol{q})\ddot{\boldsymbol{\eta}} + \left[M(\boldsymbol{q})\dot{R}(\boldsymbol{q}) + C(\boldsymbol{q},\dot{\boldsymbol{q}})R(\boldsymbol{q})\right]\dot{\boldsymbol{\eta}} + \boldsymbol{G}(\boldsymbol{q}) = B(\boldsymbol{q})\boldsymbol{\tau} + J^T(\boldsymbol{q})\boldsymbol{\lambda} \quad (8)$$

Then it is pre-multiplied (8) by $R^{\mathrm{T}}(\boldsymbol{q})$ as presented in (9).

$$R^T(\boldsymbol{q})M(\boldsymbol{q})R(\boldsymbol{q})\ddot{\boldsymbol{\eta}} + R^T(\boldsymbol{q})\left[M(\boldsymbol{q})\dot{R}(\boldsymbol{q}) + C(\boldsymbol{q},\dot{\boldsymbol{q}})R(\boldsymbol{q})\right]\dot{\boldsymbol{\eta}} + R^T(\boldsymbol{q})\boldsymbol{G}(\boldsymbol{q}) = R^{\mathrm{T}}(\boldsymbol{q})B(\boldsymbol{q})\boldsymbol{\tau} + R^{\mathrm{T}}(\boldsymbol{q})J^{\mathrm{T}}(\boldsymbol{q})\boldsymbol{\lambda} \quad (9)$$

The restriction matrix $J^T(\boldsymbol{q})\boldsymbol{\lambda}$ can be eliminated by virtue of equation (4) and is presented in (10).

$$R^T(\boldsymbol{q})M(\boldsymbol{q})R(\boldsymbol{q})\ddot{\boldsymbol{\eta}} + R^T(\boldsymbol{q})\left[M(\boldsymbol{q})\dot{R}(\boldsymbol{q}) + C(\boldsymbol{q},\dot{\boldsymbol{q}})R(\boldsymbol{q})\right]\dot{\boldsymbol{\eta}} + R^T(\boldsymbol{q})\boldsymbol{G}(\boldsymbol{q}) = R^T(\boldsymbol{q})B(\boldsymbol{q})\boldsymbol{\tau} \quad (10)$$

Consequently, we have the non-holonomic system transformed from equation (11).

$$M_1(\boldsymbol{q})\ddot{\boldsymbol{\eta}} + C_1(\boldsymbol{q},\dot{\boldsymbol{q}})\dot{\boldsymbol{\eta}} + \boldsymbol{G}_1(\boldsymbol{q}) = B_1(\boldsymbol{q})\boldsymbol{\tau} \quad (11)$$

where:

$$M_1(\boldsymbol{q}) = R^T(\boldsymbol{q})M(\boldsymbol{q})R(\boldsymbol{q})$$
$$C_1(\boldsymbol{q},\dot{\boldsymbol{q}}) = R^T(\boldsymbol{q})\left[M(\boldsymbol{q})\dot{R}(\boldsymbol{q}) + C(\boldsymbol{q},\dot{\boldsymbol{q}})R(\boldsymbol{q})\right]$$
$$\boldsymbol{G}_1(\boldsymbol{q}) = R^T(\boldsymbol{q})\boldsymbol{G}(\boldsymbol{q})$$
$$B_1(\boldsymbol{q}) = R^T(\boldsymbol{q})B(\boldsymbol{q})$$

this being more appropriate for the design of a controller, as the restriction $\boldsymbol{\lambda}$ has been removed from the dynamic equation [21], [22].

**Non-holonomic constraints. Case reported in [21]**

The mobile platform is driven by a differential system such as the one presented in the Figure 2. For ease the following notation is used in the equations: $s_m = \sin\theta_m$, $c_m = \cos\theta_m$, $s_1 = \sin\theta_1$, $c_1 = \cos\theta_1$, $s_2 = \sin\theta_2$, $c_2 = \cos\theta_2$, $s_3 = \sin\theta_3$, $c_3 = \cos\theta_3$, $s_{m1} = \sin(\theta_m + \theta_1)$, $c_{m1} = \cos(\theta_m + \theta_1)$, $s_{23} = \sin(\theta_2 + \theta_3)$, $c_{23} = \cos(\theta_2 + \theta_3)$.

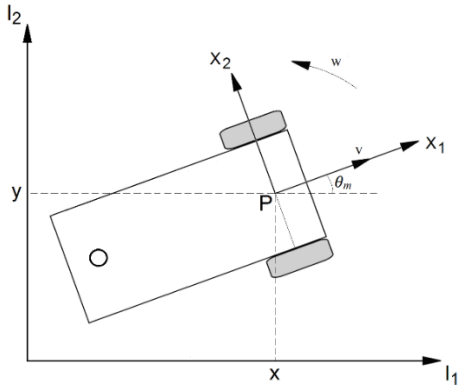


**Figure 2**. Scheme of the robot type (2.0).

If the mobile platform satisfies non-holonomic constraints (without slip), then the following constraint holds, equation (12):

$$A(\boldsymbol{q})\dot{\boldsymbol{q}} = 0 \quad (12)$$

where, $A(\boldsymbol{q}) \in \Re^{n_v \times n}$ is the matrix associated with the constraints.

The non-holonomic restriction states that the robot can only move in the direction normal to the axis of the driving wheels, that is, the mobile satisfies the conditions of pure and non-slip rolling. Therefore, the mobile platform is generally subject to three restrictions. The first being that the mobile robot cannot move in a lateral direction, see equation (13),

$$\dot{y}_o\cos\theta_m - \dot{x}_o\sin\theta_m = 0 \quad (13)$$

Since $\dot{x}_o = v\cos\theta_m$ and $\dot{y}_o = v\sin\theta_m$ where $(\dot{x}_o, \dot{y}_o)$ is the linear velocity at the center point of the driving wheels, $v$ is the velocity of the platform, and $\theta_m$ is the orientation angle of the moving robot measured from the $X$ axis. Equation (13) is a non-holonomic constraint and cannot be analytically integrated producing a constraint between platform configuration variables, i.e. $\dot{x}_o$, $\dot{y}_o$ and $\dot{\theta}_m$. The configuration space of the system is three-dimensional (completely unrestricted), while the velocity space is two-dimensional. This restriction is rewritten as observed in equations (14) and (15):

$$\dot{x}_o\cos\theta_m + \dot{y}_o\sin\theta_m + L\dot{\theta}_m = r\dot{\theta}_r \quad (14)$$
$$\dot{x}_o\cos\theta_m + \dot{y}_o\sin\theta_m - L\dot{\theta}_m = r\dot{\theta}_l \quad (15)$$

where $\dot{\theta}_r$ and $\dot{\theta}_l$ are the angular velocities of the two driving wheels, respectively, and $2L$ is the width of the platform. The generalized coordinates of the mobile platform are $\boldsymbol{q} = [\dot{x}_o \quad \dot{y}_o \quad \dot{\theta}_m \quad \dot{\theta}_r \quad \dot{\theta}_l]^T$. The three constraints lead to the matrix $A(\boldsymbol{q})$ that is presented in equation (16).

$$A(\theta_m) = \begin{bmatrix} -\sin\theta_m & \cos\theta_m & 0 & 0 & 0 \\ \cos\theta_m & \sin\theta_m & L & -r & 0 \\ \cos\theta_m & \sin\theta_m & -L & 0 & r \end{bmatrix} \quad (16)$$

where $m$ is the matrix range $R(\boldsymbol{q}) \in \Re^{n \times m}$ formed by a set of linearly independent vector fields spanning the null space of $A(\boldsymbol{q})$, as demonstrated in equation (17).

$$R^T(\boldsymbol{q})A^T(\boldsymbol{q}) = 0 \quad (17)$$

According to equations (12) and (17), it is possible to find an auxiliary vector as a function of time $\boldsymbol{v}(t) \in \Re^{n-m}$ such that, for all time $t$ give equation (18).

$$\dot{\boldsymbol{q}} = R(\boldsymbol{q})\boldsymbol{v}(t) \quad (18)$$

where $\boldsymbol{v}(t) = [\dot{\theta}_r, \dot{\theta}_l]$.

For the two-wheeled mobile robot presented in Figure 2, we can define the matrix $R(\boldsymbol{q}) \in \Re^{5\times 2}$ as expressed in equation (19):

$$R(\boldsymbol{q}) = [r_1(\boldsymbol{q}) \quad r_2(\boldsymbol{q})]\begin{bmatrix} \frac{r}{2}\cos\theta_m & \frac{r}{2}\cos\theta_m \\ \frac{r}{2}\sin\theta_m & \frac{r}{2}\sin\theta_m \\ \frac{r}{2L} & -\frac{r}{2L} \\ 1 & 0 \\ 0 & 1 \end{bmatrix} \quad (19)$$

The matrix $R(\boldsymbol{q})$ is in the null space of the matrix $A(\boldsymbol{q})$ that is, $R^T(\boldsymbol{q})A^T(\boldsymbol{q}) = 0$.

To obtain the holonomic constraint, we subtract equation (14) from equation (15), obtaining equation (20).

$$2L\dot{\theta}_m = r(\dot{\theta}_r - \dot{\theta}_l) \quad (20)$$

Integrating the above equation and choosing the initial condition of $\theta_m(0) = \theta_r(0) = \theta_l(0)$, equation (21) is obtained.

$$\theta_m = \frac{r}{2L}(\theta_r - \theta_l) \quad (21)$$

Since this equation is a holonomic constraint, $\theta_m$ can be eliminated from the generalized coordinates. The second non-holonomic constraint is found by adding equations (14) and (15). The two non-holonomic constraints are presented in equations (22) and (23):

$$\dot{x}_o\sin\theta_m - \dot{y}_o\cos\theta_m = 0 \quad (22)$$

$$\dot{x}_o\cos\theta_m + \dot{y}_o\sin\theta_m = \frac{r}{2}(\dot{\theta}_r + \dot{\theta}_l) \quad (23)$$

It is understood that $\theta_m$ is now an abbreviate notation of $c(\theta_r - \theta_l)$ instead of an independent variable. You can write these two restriction equations in the matrix form as presented in equation (24).

$$A(\boldsymbol{q})\dot{\boldsymbol{q}} = 0 \quad (24)$$

where the generalized coordinate vector $\boldsymbol{q}$ is now defined in equation (25).

$$\boldsymbol{q} = \begin{bmatrix} q_1 \\ q_2 \\ q_3 \\ q_4 \end{bmatrix} = \begin{bmatrix} x_0 \\ y_0 \\ \theta_r \\ \theta_l \end{bmatrix} \quad (25)$$

and $A(\boldsymbol{q})$ is given by (26).

$$A = \begin{bmatrix} -sin\theta_m & cos\theta_m & 0 & 0 \\ -cos\theta_m & -sin\theta_m & \frac{r}{2} & \frac{r}{2} \end{bmatrix} \quad (26)$$

**Non-holonomic constraints. Case in study**

For the mobile platform driven by a differential system as the one shown in Figure 3.a. The kinematics of the mobile platform is determined in the reference system $O_b$, because there is the base of the manipulator.

The calculation of the speeds in $X$ and $Y$ of the point $O_b$ is presented in equations (27) and (28).

$$\dot{x}_b = vc_m - v_T s_m \quad (27)$$

$$\dot{y}_b = vs_m + v_T c_m \quad (28)$$

Where $v_T$ is the tangential velocity at that point due to the angular velocity $w = \dot{\theta}_m$. Equations (27) and (28) can be expressed in terms of $w$ by means of the relationship $v_T = wd$ and in matrix form as presented in equation (29).

$$\begin{bmatrix} \dot{x}_b \\ \dot{y}_b \\ \dot{\theta}_m \end{bmatrix} = \begin{bmatrix} c_m & -ds_m \\ s_m & dc_m \\ 0 & 1 \end{bmatrix}\begin{bmatrix} v \\ w \end{bmatrix} \quad (29)$$

In Figure 3.b shows that the linear velocity of each wheel $v_r$ (right wheel) and $v_l$ (left wheel) is perpendicular to the rotation axis, so the velocity $\dot{\theta}_m$ is produced by the composition of the linear velocities of each of the wheels and the linear velocity at the Center of Mass (CM) $v_{cm} = v$ will be equally perpendicular to those of the wheels' shafts.

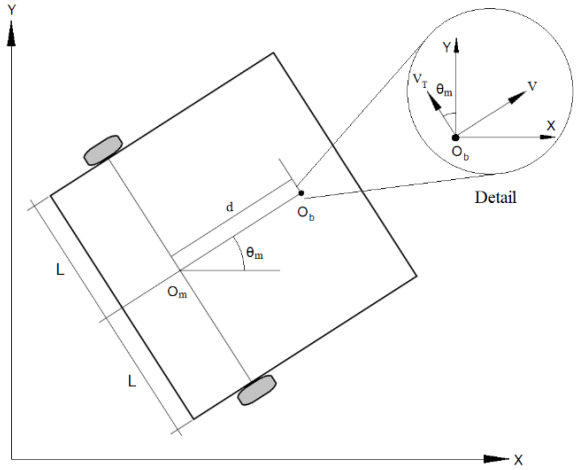


a. Robot speed at point $O_b$

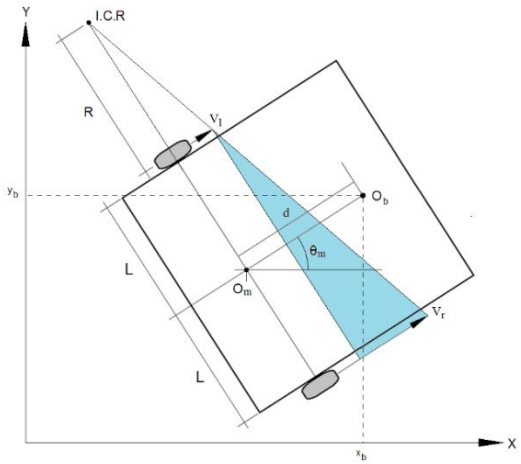


b. Robot speed in respect to point ICR

**Figure 3.** Robot speeds

As the Instant Center of Rotation (ICR) is the full mass of the mobile, the linear speed of the mobile is the product of the angular velocity of the mobile $\dot{\theta}_m$ and position of $O_m$ in respect of ICR, as presented in equation (30).

$$v = \dot{\theta}_m(R + L) \tag{30}$$

Where 2L is the length and width of the mobile and R is the distance from ICR to the nearest wheel. Therefore, the speed of each wheel is calculated by means of equations (31) and (32).

$$v_l = \dot{\theta}_m R \tag{31}$$

$$v_r = \dot{\theta}_m(R + 2L) \tag{32}$$

From Figure 3.b, we can deduce the equation (33) by means of the similarity between triangles, which relates the linear velocities of each wheel with respect to the point $O_m$.

$$\frac{v - v_l}{v_r - v_l} = \frac{L}{2L}$$
$$v = \frac{v_r + v_l}{2} \tag{33}$$

Using Figure 3.b, the relationship between the speed of each wheel at the time of producing a turn can be determined. In this way, the result is the difference in the speeds of the wheels in respect of the width of the platform $2L$ and is presented in the equation (34).

$$\dot{\theta}_m = \frac{v_r - v_l}{2L} \tag{34}$$

Expressing equations (33) and (34) in terms of $\dot{\theta}_r$ and $\dot{\theta}_l$ we have equations (35) and (36), by means of the expressions $v_r = r\dot{\theta}_r$ and $v_l = r\dot{\theta}_l$, where $r$ is the radius of the wheel.

$$v = \frac{r(\dot{\theta}_r + \dot{\theta}_l)}{2} \tag{35}$$

$$\dot{\theta}_m = \frac{r(\dot{\theta}_r - \dot{\theta}_l)}{2L} \tag{36}$$

In matrix form, it is presented in equation (37).

$$\begin{bmatrix} v \\ w \end{bmatrix} = \begin{bmatrix} \frac{r}{2} & \frac{r}{2} \\ \frac{r}{2L} & -\frac{r}{2L} \end{bmatrix} \begin{bmatrix} \dot{\theta}_r \\ \dot{\theta}_l \end{bmatrix} \tag{37}$$

Finally, the product of the matrices (29) and (37) is made and the result is presented in equation (38).

$$\begin{bmatrix} \dot{x}_b \\ \dot{y}_b \\ \dot{\theta}_m \\ \dot{\theta}_r \\ \dot{\theta}_l \end{bmatrix} = \begin{bmatrix} \frac{r}{2L}(Lc_m - ds_m) & \frac{r}{2L}(Lc_m + ds_m) \\ \frac{r}{2L}(Ls_m + dc_m) & \frac{r}{2L}(Ls_m - dc_m) \\ \frac{r}{2L} & -\frac{r}{2L} \\ 1 & 0 \\ 0 & 1 \end{bmatrix} \begin{bmatrix} \dot{\theta}_r \\ \dot{\theta}_l \end{bmatrix} \tag{38}$$

**Inverse coupled dynamics of the MM**

In this section, the coupled inverse dynamic modeling of the MM is performed. As mentioned before, the purpose of this article is to perform the dynamic coupling of the MM using a generalized formulation and including non-holonomic restrictions of the mobile platform. Therefore, the Lagrange formulation is used because it can be carried out in a general manner. It begins by determining the location in $X$, $Y$ and $Z$ of the elements that are listed in Table 1 with its corresponding nomenclature (the hyphen indicates that the parameter is not variant in time and therefore is not considered in the dynamic).

**Table 1.** Nomenclature for the location of MM elements.

| Item | Position in X | Position in Y | Position in Z |
|---|---|---|---|
| CM of the right wheel | $x_{cm_r}$ | $y_{cm_r}$ | – |
| CM of the left wheel | $x_{cm_l}$ | $y_{cm_l}$ | – |
| Mobile mass center | $x_{cm_m}$ | $y_{cm_m}$ | – |
| CM of the link 1 | $x_{cm_1}$ | $y_{cm_1}$ | – |
| CM of the link 2 | $x_{cm_2}$ | $y_{cm_2}$ | $z_{cm_2}$ |
| CM of the link 3 | $x_{cm_3}$ | $y_{cm_3}$ | $z_{cm_3}$ |

To determine the positions, Figure 4, Figure 5 and Figure 6 are used, which present the robot in the X-Y and X-Z planes. To determine the dynamic the follow nomenclature is used:

$m_i$ Mass of the element $i$
$L_{cmx_i}$ Distance in X of CM to origin of the element $i$
$L_i$ Link length $i$
$I_{xx_i}$ Inertia of the element $i$ in respect of axis X
$I_{yy_i}$ Inertia of the element $i$ in respect of axis $Y$
$I_{zz_i}$ Inertia of the element $i$ in respect of axis $Z$

In the subscript $i$ is used $r$ to indicate right wheel, $l$ to indicate left wheel, $w$ to indicate wheel, $m$ to indicate mobile platform and *1,2* and *3* to indicate the number of link.

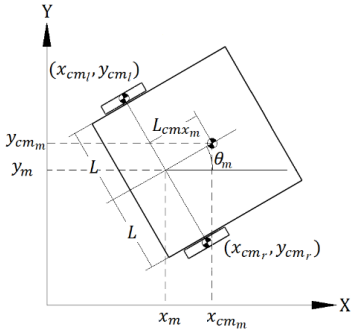


**Figure 4.** View of the MM in the X-Y plane.

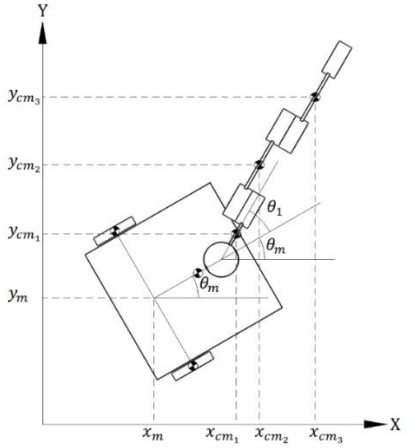


**Figure 5.** View of the MM in the X-Y plane.

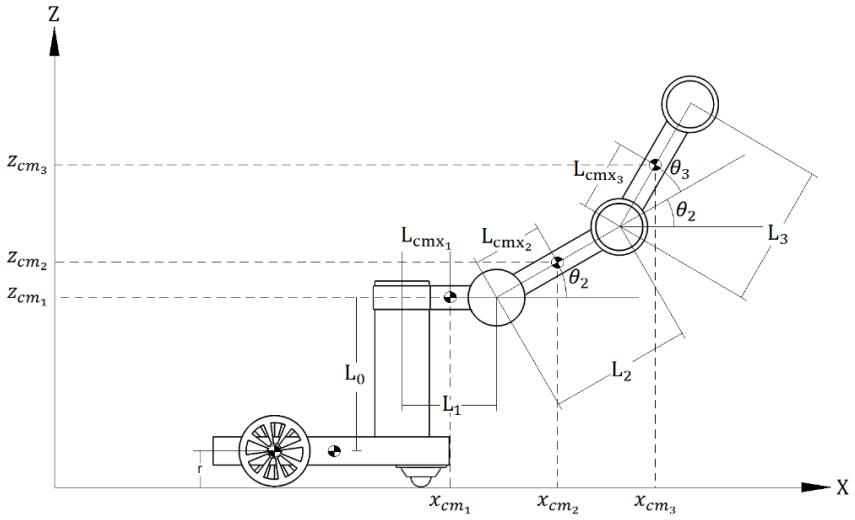


**Figure 6.** View of the MM in the X-Z plane.

From equation (39) to (52) the positions of the bodies that make up the robot are presented; these equations are used to determine the kinetic and potential energy of the system.

$$x_{cm_r} = x_m + Ls_m \tag{39}$$
$$y_{cm_r} = y_m - Lc_m \tag{40}$$
$$x_{cm_l} = x_m - Ls_m \tag{41}$$
$$y_{cm_l} = y_m + Lc_m \tag{42}$$
$$x_{cm_m} = x_m + L_{cmx_m}c_m \tag{43}$$
$$y_{cm_m} = y_m + L_{cmx_m}s_m \tag{44}$$
$$x_{cm_1} = x_m + dc_m + L_{cmx_1}c_{m1} \tag{45}$$
$$y_{cm_1} = y_m + ds_m + L_{cmx_1}s_{m1} \tag{46}$$
$$x_{cm_2} = x_m + dc_m + L_1c_{m1} + (L_{cmx_2}c_2)c_{m1} \tag{47}$$
$$y_{cm_2} = y_m + ds_m + L_1s_{m1} + (L_{cmx_2}c_2)s_{m1} \tag{48}$$
$$z_{cm_2} = r + L_0 + L_{cmx_2}s_2 \tag{49}$$
$$x_{cm_3} = x_m + dc_m + L_1c_{m1} + (L_2c_2)c_{m1} + (L_{cmx_3}c_{23})c_{m1} \tag{50}$$
$$y_{cm_3} = y_m + ds_m + L_1s_{m1} + (L_2c_2)s_{m1} + (L_{cmx_3}c_{23})s_{m1} \tag{51}$$
$$z_{cm_3} = r + L_0 + L_2s_2 + L_{cmx_3}s_{23} \tag{52}$$

The velocities of each body are presented in the equations (53) to (66).

$$\dot{x}_{cm_r} = \dot{x}_m + Lc_m\dot{\theta}_m \tag{53}$$
$$\dot{y}_{cm_r} = \dot{y}_m + Ls_m\dot{\theta}_m \tag{54}$$
$$\dot{x}_{cm_l} = \dot{x}_m - Lc_m\dot{\theta}_m \tag{55}$$
$$\dot{y}_{cm_l} = \dot{y}_m - Ls_m\dot{\theta}_m \tag{56}$$
$$\dot{x}_{cm_m} = \dot{x}_m - L_{cmx_m}s_m\dot{\theta}_m \tag{57}$$
$$\dot{y}_{cm_m} = \dot{y}_m + L_{cmx_m}c_m\dot{\theta}_m \tag{58}$$
$$\dot{x}_{cm_1} = \dot{x}_m - ds_m\dot{\theta}_m - L_{cmx_1}s_{m1}(\dot{\theta}_m + \dot{\theta}_1) \tag{59}$$
$$\dot{y}_{cm_1} = \dot{y}_m + dc_m\dot{\theta}_m + L_{cmx_1}c_{m1}(\dot{\theta}_m + \dot{\theta}_1) \tag{60}$$
$$\dot{x}_{cm_2} = \dot{x}_m - ds_m\dot{\theta}_m - L_1s_{m1}(\dot{\theta}_m + \dot{\theta}_1) - L_{cmx_2}s_2\dot{\theta}_2c_{m1} - L_{cmx_2}c_2s_{m1}(\dot{\theta}_m + \dot{\theta}_1) \tag{61}$$
$$\dot{y}_{cm_2} = \dot{y}_m + dc_m\dot{\theta}_m + L_1c_{m1}(\dot{\theta}_m + \dot{\theta}_1) - L_{cmx_2}s_2\dot{\theta}_2s_{m1} + L_{cmx_2}c_2c_{m1}(\dot{\theta}_m + \dot{\theta}_1) \tag{62}$$
$$\dot{z}_{cm_2} = L_{cmx_2}c_2\dot{\theta}_2 \tag{63}$$
$$\dot{x}_{cm_3} = \dot{x}_m - ds_m\dot{\theta}_m - L_1s_{m1}(\dot{\theta}_m + \dot{\theta}_1) - L_2s_2\dot{\theta}_2c_{m1} - L_2c_2s_{m1}(\dot{\theta}_m + \dot{\theta}_1) - L_{cmx_3}s_{23}(\dot{\theta}_2 + \dot{\theta}_3)c_{m1} - L_{cmx_3}c_{23}s_{m1}(\dot{\theta}_m + \dot{\theta}_1) \tag{64}$$
$$\dot{y}_{cm_3} = \dot{y}_m + dc_m\dot{\theta}_m + L_1c_{m1}(\dot{\theta}_m + \dot{\theta}_1) - L_2s_2\dot{\theta}_2s_{m1} + L_2c_2c_{m1}(\dot{\theta}_m + \dot{\theta}_1) - L_{cmx_3}s_{23}(\dot{\theta}_2 + \dot{\theta}_3)s_{m1} + L_{cmx_3}c_{23}c_{m1}(\dot{\theta}_m + \dot{\theta}_1) \tag{65}$$
$$\dot{z}_{cm_3} = L_2c_2\dot{\theta}_2 + L_{cmx_3}c_{23}(\dot{\theta}_2 + \dot{\theta}_3) \tag{66}$$

The kinetic and potential energy of each body are presented from equation (67) to (77).

$$K_r = \frac{1}{2}m_w\left(\dot{x}_{cm_d}{}^2 + \dot{y}_{cm_d}{}^2\right) + \frac{1}{2}I_{yy_w}\dot{\theta}_m^2 + \frac{1}{2}I_{zz_w}\dot{\theta}_d^2 \tag{67}$$
$$K_l = \frac{1}{2}m_w\left(\dot{x}_{cm_i}{}^2 + \dot{y}_{cm_i}{}^2\right) + \frac{1}{2}I_{yy_w}\dot{\theta}_m^2 + \frac{1}{2}I_{zz_w}\dot{\theta}_l^2 \tag{68}$$
$$K_m = \frac{1}{2}m_m\left(\dot{x}_{cm_m}{}^2 + \dot{y}_{cm_m}{}^2\right) + \frac{1}{2}I_m\dot{\theta}_m^2 \tag{69}$$
$$K_1 = \frac{1}{2}m_1\left(\dot{x}_{cm_1}{}^2 + \dot{y}_{cm_1}{}^2\right) + \frac{1}{2}I_{zz_1}(\dot{\theta}_m + \dot{\theta}_1)^2 \tag{70}$$
$$K_2 = \frac{1}{2}m_2\left(\dot{x}_{cm_2}{}^2 + \dot{y}_{cm_2}{}^2 + \dot{z}_{cm_2}{}^2\right) + \frac{1}{2}I_{zz_2}(\dot{\theta}_m + \dot{\theta}_1)^2 + \frac{1}{2}I_{yy_2}\dot{\theta}_2^2 \tag{71}$$
$$K_3 = \frac{1}{2}m_3\left(\dot{x}_{cm_3}{}^2 + \dot{y}_{cm_3}{}^2 + \dot{z}_{cm_3}{}^2\right) + \frac{1}{2}I_{zz_3}(\dot{\theta}_m + \dot{\theta}_1)^2 + \frac{1}{2}I_{yy_3}(\dot{\theta}_2 + \dot{\theta}_3)^2 \tag{72}$$
$$U_r = 0 \tag{73}$$
$$U_l = 0$$
$$U_m = 0 \tag{74}$$
$$U_1 = 0 \tag{75}$$
$$U_2 = -m_2g\left(L_0 + L_{cmx_2}s_2\right) \tag{76}$$
$$U_3 = -m_3g\left(L_0 + L_2s_2 + L_{cmx_3}s_{23}\right) \tag{77}$$

The dynamic model of the system is obtained applying the Lagrange formula presented in equation (11), to obtain the model under non-holonomic constraints, we use the matrix $R(\boldsymbol{q}) \in \Re^{n\times m}$ that shown in equation (38). The mathematical development of the Lagrange equation was done in Maple®.

**Results**

To validate the obtained model, a simulation was carried out in Simulink of Matlab®. In this simulation the Simscape Multibody™ tool was used to loading the mechanic model of the MM designed in SolidWorks®. The inclusion of mechanical design allows the simulation to be more real and reliable, since the physical properties (mass, inertia, etc.) of each robot body are considered.

The values of the physical parameters that are used in the simulation, and that come from the design made in SolidWorks, are presented in Table 2.

**Table 2.** Values of the physical parameters.

| Symbol | Value | Units | Symbol | Value | Units |
|---|---|---|---|---|---|
| $L$ | 0.250 | $m$ | $L_{cmx_2}$ | 0.246 | $kg.m^2$ |
| $d$ | 0.270 | $m$ | $L_{cmx_3}$ | 0.150 | $kg.m^2$ |
| $m_m$ | 19.2372 | $kg$ | $m_1$ | 3.293 | $kg$ |
| $I_m$ | 0.7004 | $kg.m^2$ | $m_2$ | 3.436 | $kg$ |
| $r$ | 0.075 | $m$ | $m_3$ | 1.229 | $kg$ |
| $L_{cmx_m}$ | 0.2268 | $m$ | $I_{xx_1}$ | 0.0053 | $kg.m^2$ |
| $m_w$ | 0.901 | $kg$ | $I_{yy_1}$ | 0.0221 | $kg.m^2$ |
| $I_{yy_w}$ | 0.0015 | $kg.m^2$ | $I_{zz_1}$ | 0.0230 | $kg.m^2$ |
| $I_{zz_w}$ | 0.0030 | $kg.m^2$ | $I_{xx_2}$ | 0.0054 | $kg.m^2$ |
| $L_0$ | 0.325 | $m$ | $I_{yy_2}$ | 0.0457 | $kg.m^2$ |
| $L_1$ | 0.200 | $m$ | $I_{zz_2}$ | 0.0461 | $kg.m^2$ |
| $L_2$ | 0.300 | $m$ | $I_{xx_3}$ | 0.0017 | $kg.m^2$ |
| $L_3$ | 0.300 | $m$ | $I_{yy_3}$ | 0.0242 | $kg.m^2$ |
| $L_{cmx_1}$ | 0.167 | $kg.m^2$ | $I_{zz_3}$ | 0.0255 | $kg.m^2$ |

The values of the movement parameters that are used in the simulation are presented in the Table 3.

**Table 3.** Values of the movement parameters.

| | Initial position | Final position |
|---|---|---|
| Right wheel [mm] | 600 | -600 |
| Left wheel [mm] | 600 | -600 |
| Link 1 [°] | 0 | 90 |
| Link 2 [°] | -90 | 90 |
| Link 3 [°] | 90 | -90 |

In Figure 7 the torque behavior of each joint when performing the movement can be seen.

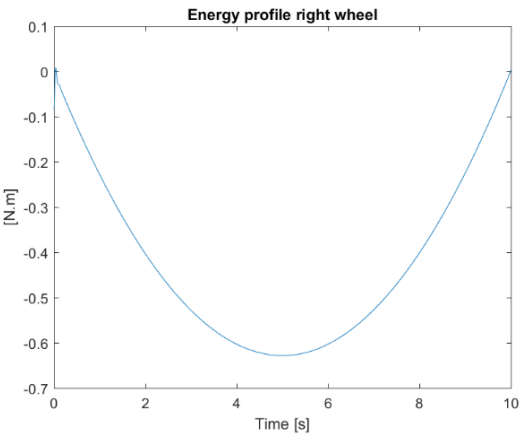


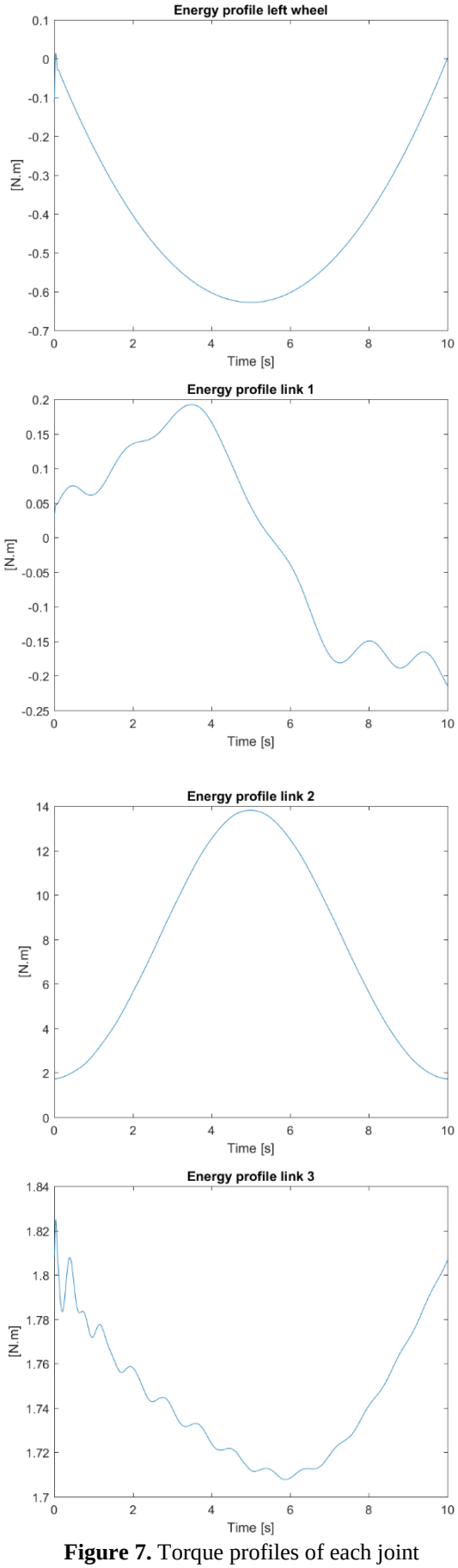


**Figure 7.** Torque profiles of each joint

**Conclusions**

The torque profiles show that there is an interaction in each of the joints, that is, when a movement of one of the joints is made, the others see the effect of this movement, mainly with the presence of vibrations. This can also be evidenced in the terms of the dynamic model's inertia and velocity matrix, where you can see sums of velocity and inertial terms of each body in a single expression.

The emphasis of this paper has been set on obtaining precise and complete equations of motion, which includes the simultaneous rotating, the non-holonomic constraints associated with the dynamic interactions between the manipulator and the mobile platform. The advantage of having the coupled dynamic model of MM lies in the fact that coordinated movements of the base can be programmed with the manipulator and in turn avoid inappropriate positions that involve overturning or collisions with the same structure.

As a future work, it is desired to develop the control of the coupled dynamic model of the MM to implement optimization techniques to guarantee the minimum energy consumption.

**Acknowledgment**

The authors thank the Instituto Politecnico Nacional (Mexico) for its support through the Research and Postgraduate Secretariat. Prada-Jiménez V. thanks CONACYT (Mexico) and the Universidad Central (Colombia) for their support in the doctorate studies commission.

**References**

[1] A. K. Solutions, *Robotics*. Infinity Science Press, 2007.

[2] A. Ollero, *Robótica. Manipuladores y robots móviles.* Marcombo, 2001.

[3] O. Ibrahim and W. Khalil, "Inverse and direct dynamic models of hybrid robots," *Mech. Mach. Theory*, vol. 45, no. 4, pp. 627–640, Apr. 2010.

[4] G. B. Chung, B.-J. Yi, D. J. Lim, and W. Kim, "An efficient dynamic modeling methodology for general type of hybrid robotic systems," *IEEE Int. Conf. Robot. Autom. 2004. Proceedings. ICRA 2004*, vol. 2, pp. 1795–1802, 2004.

[5] P. Ben-Tzvi, A. A. Goldenberg, and J. W. Zu, "Design and Analysis of a Hybrid Mobile Robot Mechanism With Compounded Locomotion and Manipulation Capability," *J. Mech. Des.*, vol. 130, no. 7, p. 072302, 2008.

[6] P. M. Escobedo, "Manipulador móvil: Estudio sobre la coordinación de movimientos de un manipulador serial acoplado," Universidad Nacional Autónoma de México, 2012.

[7] G. Campion, G. Bastin, and B. Dandrea-Novel, "Structural properties and classification of kinematic and dynamic models of wheeled mobile robots," *IEEE Trans. Robot. Autom.*, vol. 12, no. 1, pp. 47–62, 1996.

[8] Y. Yamamoto and X. Yun, "Coordinating locomotion and manipulation of a mobile manipulator," *Gen. Robot. Act. Sens. Percept. Lab.*, no. December, pp. 2643–2648, 1992.

[9] Z. Li, W. Chen, and H. Liu, "Robust Control of Wheeled Mobile Manipulators Using Hybird Joints," *Int. J. Adv. Robot. Syst.*, vol. 5, no. 1, pp. 83–90, 2008.

[10] N. A. M. Hootsmans, "The motion control of manipulators on mobile vehicles," Massachusetts Institute of Technology, 1992.

[11] D. Naderi, A. Meghdari, and M. Durali, "Dynamic modeling and analysis of a two d.o.f. mobile manipulator," *Robotica*, vol. 19, no. 2001, pp. 177–185, 2001.

[12] G. H. Salazar Silva, M. A. Moreno Armendáriz, and J. Álvarez Gallegos, "Modelado y control de un manipulador móvil en el espacio de la tarea," Instituto Politecnico Nacional, 2013.

[13] H. G. Tanner and K. J. Kyriakopoulos, "Mobile manipulator modeling with Kane's approach," *Robotica*, vol. 19, no. 2001, pp. 675–690, 2017.

[14] H. G. Tanner, K. J. Kyriakopoulos, and N. I. Krikelis, "Advanced agricultural robots: kinematics and dynamics of multiple mobile manipulators handling non-rigid material," *Elsevier*, vol. 31, pp. 91–105, 2001.

[15] J. I. Nantes, R. Carelli, I. De Automática, and U. Nacional, "Control coordinado de un manipulador móvil con evasión de obstáculos y máxima manipulabilidad," in *V Jornadas Argentinas de Robótica*, 2008.

[16] S. N. Mostafa, G. Mostafa, and M. Masoud, "Optimal Trajectory Planning of a Mobile Robot with Spatial Manipulator For Obstacle Avoidance," *Int. Conf. Control. Autom. Syst. 2010*, pp. 314–318, 2010.

[17] C. A. My and L. C. Thanh, "Inverse Dynamic of a N-links Manipulator Mounted on a Wheeled Mobile Robot," *ICCAIS 2013*, pp. 164–170, 2013.

[18] X. Yun and Y. Yamamoto, "Internal dynamics of a wheeled mobile robot," *Proc. 1993 IEEE/RSJ Int. Conf. Intell. Robot. Syst. (IROS '93)*, vol. 2, no. C, pp. 1288–1294, 1993.

[19] R. Miranda Colorado, *Cinemática y dinámica de robots manipuladores*. Alfaomega, 2016.

[20] F. Reyes Cortés, *Robótica. Control de Robots Manipuladores*. Alfaomega, 2011.

[21] Z. Li and S. S. Ge., *Fundamentals in Modeling and Control of Mobile Manipulators*. CRC Press, 2013.

[22] S. G. Tzafestas, "Mobile Manipulator Modeling and Control," in *Introduction to Mobile Robot Control*, Elsevier, 2014, pp. 385–428.

[23] A. Bañó Azcon, "Análisis y diseño del control de posición de un robot móvil con tracción diferencial," Escola Tecnica Superior Enginyeria, 2003.